8416–8429 *Nucleic Acids Research, 2011, Vol. 39, No. 19* *Published online 10 July 2011*
doi:10.1093/nar/gkr463

Post-irradiation chemical processing of DNA damage generates double-strand breaks in cells already engaged in repair

Satyendra K. Singh, Minli Wang, Christian Staudt and George Iliakis*

Institute of Medical Radiation Biology, University of Duisburg-Essen Medical School, 45122 Essen, Germany

Received February 1, 2011; Revised May 18, 2011; Accepted May 19, 2011

ABSTRACT

In cells exposed to ionizing radiation (IR), double-strand breaks (DSBs) form within clustered-damage sites from lesions disrupting the DNA sugar–phosphate backbone. It is commonly assumed that these DSBs form promptly and are immediately detected and processed by the cellular DNA damage response (DDR) apparatus. This assumption is questioned by the observation that after irradiation of naked DNA, a fraction of DSBs forms minutes to hours after exposure as a result of temperature dependent, chemical processing of labile sugar lesions. Excess DSBs also form when IR-exposed cells are processed at 50°C, but have been hitherto considered method-related artifact. Thus, it remains unknown whether DSBs actually develop in cells after IR exposure from chemically labile damage. Here, we show that irradiation of 'naked' or chromatin-organized mammalian DNA produces lesions, which evolve to DSBs and add to those promptly induced, after 8–24 h *in vitro* incubation at 37°C or 50°C. The conversion is more efficient in chromatin-associated DNA, completed within 1 h in cells and delayed in a reducing environment. We conclude that IR generates sugar lesions within clustered-damage sites contributing to DSB formation only after chemical processing, which occurs efficiently at 37°C. This subset of delayed DSBs may challenge DDR, may affect the perceived repair kinetics and requires further characterization.

INTRODUCTION

Sparsely ionizing radiation (IR) deposits energy in the form of spatially distinct single ionization events, as well as in the form of ionization clusters of different sizes (1). These events alter the DNA molecule either through direct ionization, or indirectly through the production of water radicals, which quickly react with and damage proximal DNA. Radiation-induced, chemical DNA alterations are classified as base damage (or loss), or sugar damage (accompanied or not by base loss) (2,3). Typically, base damage does not structurally alter the DNA molecule, and the sugar-phosphate backbone is opened as a programmed event during base excision repair (4).

Sugar lesions, on the other hand, frequently disrupt promptly the sugar-phosphate backbone and generate DNA single-strand breaks (SSBs) (2,3). Since sugar lesions are induced in random combinations within clustered-damage sites (CDS), their simultaneous presence in opposite DNA strands within one helical turn will lead to the formation of DNA double-strand breaks (DSBs) (1,5–9). The efficient induction of DSBs by IR is the direct consequence of this clustering of ionization events and a presumed prompt breakage of the sugar–phosphate backbone. Since DSBs fragment the genome, they must be repaired efficiently to prevent genomic alterations causing mutations or chromosome aberrations that can ultimately lead to cell death or cancer.

The severity of the DSB as a DNA lesion is clearly documented by the highly elaborate cellular responses it initiates and which are commonly integrated under the term DNA damage response (DDR) (10). DDR is equipped to detect DSBs and co-ordinate their repair, on the basis of internal and external signals, with the

*To whom correspondence should be addressed. Tel: +49 201 723 4152, Fax: +49 201 723 5966; Email: georg.Iliakis@uk-essen.de
Present addresses:
Dr. S.K. Singh. Mouse Cancer Genetics ProgramNCI-Frederick, Frederick, Maryland, 21702, USA
Dr. M. Wang. NASA-JSC Space Radiation Health Project, Bldg 37, R119, 2010 NASA Parkway, Houston, TX-77058, USA
Dr. C. Staudt. Helmholtz Zentrum München GmbH, Ingolstädter Landstraße 1, 85764 Neuherberg, Germany

The authors wish it to be known that, in their opinion, the first two authors should be regarded as joint First Authors.

cellular machineries of DNA transcription, DNA replication, cell cycle and apoptosis (10).

Analysis of DDR after IR and, in particular, analysis of DSB repair kinetics are generally based on the assumption that DSBs form promptly and are detectable in the cell, in their entirety, immediately after completion of radiation exposure. However, early work carried out with plasmid DNA raises questions regarding the general validity of this assumption. Thus, experiments with *in vitro* irradiated DNA showed that the yield of DSBs depends strongly on post-irradiation conditions such as temperature and pH (11–13). As a result, DSB yields recorded with DNA irradiated and analyzed at 4°C, nearly double upon incubation for several hours at 20°C; they increase further at 37°C without evidence for a plateau even after 18 h of incubation (12).

These results suggest that IR also induces, in addition to sugar lesions directly disrupting the sugar–phosphate backbone (prompt breaks), lesions doing so after temperature-dependent chemical processing (delayed breaks). Based on such observations, three forms of sugar lesions have been proposed to form in irradiated DNA (12): (i) free deoxyribose products with both phosphodiester bonds broken and an unaltered base released; (ii) altered sugars bound by one phosphodiester bond to a broken DNA strand and the unaltered base released; and (iii) fragmented and/or oxidized sugars with both phosphodiester bonds still intact and with the base released or not. While the first two types of sugar lesions cause direct strand breakage, the latter form constitutes what is considered radiation-induced labile sites—because they can evolve to breaks by post-irradiation chemical modification (1,7,12).

While the nature of labile lesions remains elusive, they are likely to represent oxidative sugar damage (3,14). However, their evolution to lesions disrupting DNA continuity contributes to delayed DSB formation when present within a CDS (6,11–13,15). The observation that cellular repair is compromised within a CDS (8,9,16,17), increases the time-window for DSB formation from such lesion interactions—should such lesions form not only in irradiated DNA but also in irradiated cells.

Extrapolation of the above *in vitro* observations to cells raises the possibility of delayed induction of DSBs during the post-irradiation incubation interval at 37°C, where exclusively repair is thought to take place. Such delayed induction of DSBs would require revision of the widely held assumption of prompt induction of DSBs in cells exposed to IR. It is therefore surprising that the above *in vitro* observations did not receive the due notice even in the development of methods quantitating DSBs in irradiated cells. Thus, essentially all methods sizing the DNA molecule to estimate DSBs emphasize effective clean-up from associated proteins, typically achieved by extensive lysis at 50°C (18).

This limitation of the assays was elegantly demonstrated in studies published from the laboratories of Rydberg (19) and Stenerlöw *et al*. (20). By developing protocols lysing cells at 4°C as efficiently as standard 50°C lysis, these investigators convincingly demonstrated the presence immediately after irradiation of labile lesions, which contribute to excess DSB formation during lysis at 50°C. It was assumed, however, that chemical processing of these labile lesions only occurs at 50°C, and that these excess DSBs will never be generated in cells maintained for repair at 37°C—instead lesions constituting the CDS will be removed individually by non-DSB repair pathways (20,21).

Low temperature lysis (LTL) protocols showed that the yield of DSBs measured in cells immediately after IR exposure is overestimated. However, when applied to the analysis of DSB repair kinetics in mutants deficient in the DNA-PK-dependent pathway of NHEJ (D-NHEJ) (20,21), they detected severely compromised repair 2–4 h after IR. Defects of this magnitude are not in line with other phenotypic characteristics of these mutants, including the independently documented operation of robust alternative pathways of DSB repair functioning as backup (22–28). In an effort to elucidate this apparent contradiction, we studied B-NHEJ using LTL protocols (26). This work showed a robust function of B-NHEJ when LTL is carried out >2 h after IR. However, the results also showed aberrant DSB repair kinetics between 0 and 2 h after IR that did not appear compatible with results obtained using other endpoints. To resolve this discrepancy, we hypothesized the formation in irradiated cells of labile DNA lesions, which are chemically processed and form DSBs during the post-irradiation repair incubation interval (26).

Here, we outline the results of experiments that were specifically designed to test this hypothesis. We provide evidence that indeed IR induces thermally unstable DNA lesions which evolve, possibly by oxidation, to SSBs and contribute to DSB formation at physiological temperatures. We further show that this conversion is more efficient in intact cells than in 'naked' DNA, is completed within ~1 h and leads to total DSB yields similar to those measured after high temperature lysis (HTL). We propose that this subset of delayed DSBs, adds during the first post-irradiation hour to those promptly induced and repaired, alters the overall repair kinetics, particularly of D-NHEJ deficient cells, and may challenge with its inherent characteristics the DDR apparatus.

MATERIALS AND METHODS

Cell lines and culture conditions

M059K, a repair proficient human glioma cell line and *M059J* a DNA-PKcs deficient counterpart (29), were grown in Dulbecco's Modified Eagle's Minimum Essential Medium (D-MEM) supplemented with 10% fetal bovine serum (FBS), 1% non-essential amino acids and 1% L-glutamine. Mouse embryonic fibroblasts (MEFs) from $LIG4^{-/-}/p53^{-/-}$ mice (a gift of Dr F. Alt, Boston, MA, USA) (30) and from $Ku70^{-/-}$ mice (31) (a gift of Dr D. Chen, UT Southwestern Medical Center, Dallas, TX, USA) are D-NHEJ deficient and were grown in D-MEM supplemented with 10% FBS and antibiotics. CHO cells were grown in McCoy's 5A medium.

For experiments, cells were maintained in the exponential phase of growth by routine subculture at 37°C in a humidified incubator, in an atmosphere of 5% CO_2 and 95% air.

Pulsed-field gel electrophoresis

To analyze induction of DSBs, asynchronous cultures or populations enriched by centrifugal elutriation (see below) in G1 or G2-phase cells were used. Cells were re-suspended in serum free, HEPES-buffered medium at a concentration of 6×10^6 and 3×10^6 cells/ml for G1 or asynchronous and G2 cells, respectively. Cells were then mixed with an equal volume of pre-warmed 1% low melting agarose (Bio-Rad) and the cell suspension was pipetted into 3 mm diameter cylindrical glass tubes and allowed to solidify in ice. Agarose was extruded from the glass tube and cut into 5-mm long blocks, which were irradiated in a 60 mm Petri dish in 5 ml serum-free medium.

Irradiations were carried out on ice (except for the γ-H2AX experiments) with a Seifert-Pantak X-ray machine operated at 320 kV, 10 mA with a 1.65 mm Al filter (effective photon energy, ~90 kV), at a dose rate of 3 Gy/min, at a distance of 50 cm. Transfers of cells or agarose blocks to the temperature indicated by the experimental protocol was rapidly achieved with pre-warmed medium. In some experiments, cells were lysed before irradiation using the LTL protocol described below (20). In other experiments, cells embedded in agarose blocks were irradiated and, subsequently, lysed by LTL.

In the standard, HTL protocol (32), agarose blocks were placed in lysis buffer (10 mM Tris–HCl, pH 7.6, 50 mM NaCl, 100 mM EDTA, 2% *N*-lauryl sarcosyl (NLS) and 0.2 mg/ml protease added just before use) at 4°C. After 1 h incubation at this temperature, samples were transferred to 50°C for 16–18 h. Subsequently, agarose blocks were washed for 1 h at 37°C in washing buffer (10 mM Tris–HCl, 50 mM NaCl, 100 mM EDTA, pH 7.6) under constant agitation and were treated for 1 h at 37°C in a buffer containing 10 mM Tris–HCl, pH 7.6, 50 mM NaCl, 100 mM EDTA and 0.1 mg/ml freshly added RNaseA.

LTL was carried out using a published protocol (20). Agarose blocks were first transferred to 10 block volumes of ESP (EDTA, Sarkosyl, Protease) lysis buffer at 4°C (0.5 M EDTA, pH 8.0, supplemented with 2% NLS and 1 mg/ml protease, both added just before use) and were incubated at 4°C for 24 h. Subsequently, agarose blocks were transferred to 20 block volumes of high-salt buffer (4 mM Tris, pH 7.5, 1.85 M NaCl, 0.15 M KCl, 5 mM $MgCl_2$, 2 mM EDTA and 0.5% Triton X-100 added just before use) and incubated overnight (~16 h) at 4°C. Agarose blocks were washed twice for 1 h in 0.1 M EDTA, once for 1 h in TEN buffer (10 mM Tris–HCl, pH 7.5, 2 mM EDTA, 50 mM NaCl) and once for 1 h in 0.5× TBE, all at 4°C, prior to pulsed-field gel electrophoresis (PFGE).

Asymmetric Field Inversion Gel Electrophoresis (AFIGE) was carried out in gels cast with 0.5% molecular biology grade agarose (Bio-Rad) in the presence of 0.5 μg/ml ethidium bromide. Blocks were loaded into the wells of chilled (4°C) gels and were run in 0.5× TBE for 40 h at 8°C. During this time, cycles of 50 V (1.25 V/cm) for 900 s in the direction of DNA migration alternated with cycles of 200 V (5.0 V/cm) for 75 s in the reverse direction. Gels were scanned using the 'Typhoon' (GE Healthcare) and the fraction of DNA or Activity released (FAR, FDR) out of the well into the lane was quantified from images obtained using ImageQuant 5.2 (GE Healthcare). Other details have been described previously (32).

Treatments for the development of DSBs from thermally unstable radiation lesions

To monitor the kinetics of excess DSB formation at different temperatures, cells embedded in agarose blocks were exposed to IR, subjected to LTL, washed once for 1 h in TEN buffer (0.5 ml/plug) and distributed in different tubes in the same buffer. Tubes were then transferred to water baths adjusted at different temperatures ranging between 10°C and 50°C and incubated for different times before washing once in 0.5× TBE for PFGE.

To study the role of protein in the chemical development of radiation lesions, irradiated cells embedded in agarose blocks were transferred to TEN buffer supplemented with 0.2% Triton X-100 and incubated at the different temperatures for different periods of time (33). This treatment was followed by LTL and PFGE.

Throughout the article we refer to the generation of DSBs from thermally unstable lesions. Implicit in this terminology is that at least one of the SSBs that constitute the DSB derives from a thermally unstable lesion. Strictly speaking, a thermally unstable sugar lesion will only generate a SSB, and it is likely that there are many more thermally unstable lesions in DNA than DSBs forming from their conversion to SSBs.

Formamidopyrimidine [fapy]-DNA glycosylase (Fpg) and Endonuclease III (Nth) treatment

The presence of base damages within CDS transforming to DSBs was studied by treatment of irradiated DNA with Fpg or Nth (8,16,17,34). Fpg acts as *N*-glycosylase and AP-lyase Apurinic/Apyrimidinic. The *N*-glycosylase activity releases damaged purines from double-stranded DNA, generating an apurinic site. The AP-lyase activity cleaves both 3′ and 5′ to the AP site thereby removing the AP site and leaving a one-base gap. Nth from *Escherichia coli* also acts as both *N*-glycosylase and AP-lyase, but releases only damaged pyrimidines from double-stranded DNA. The AP-lyase activity cleaves 3′ to the AP site leaving a 5′ phosphate and a 3′ ring opened sugar. Irradiated and non-irradiated DNA obtained by LTL of cells embedded in agarose (~1.2 μg DNA per plug) was treated for 24 h at 20°C with Fpg (400 ng, New England Biolabs, M0240 L) in the buffer provided by the manufacturer, or Nth (1.2 μg, NEB, M0268 L) in a buffer [70 mM HEPES/KOH pH 7.6, 100 mM KCl, 1 mM EDTA, 1 mM dithiothreitol (DTT) and 50 μg/ml bovine serum albumin] reducing non-specific nuclease activity (35). After enzyme treatment agarose blocks were incubated at 20°C for 2 h with 1 mg/ml protease in TEN-buffer and washed once in TEN-buffer before PFGE.

Centrifugal elutriation

Cells ($1.4–2 \times 10^8$) were collected and elutriated at 4°C using a Beckman JE-6 elutriation rotor and a Beckman J2-21 M high speed centrifuge (Beckman-Coulter, Krefeld, Germany) in culture media supplemented with 1% serum at a flow rate of 25 ml/min (33). Cells were loaded to the rotor at 3000 rpm, and 250 ml fractions were collected between 2500 and 1500 rpm at 100 rpm steps. During elutriation cells of small size, typically representing the G1 subpopulation, leave the rotor first, while larger cells, representing populations enriched in S and G2, leave the rotor in subsequent fractions. In this way cell populations highly enriched in G1 and G2 are obtained for experiments. Cell cycle analysis was carried out by flow cytometry.

Laser scanning confocal microscopy

For immunofluorescence staining, cells were grown after elutriation for 1 h at 37°C on poly-L-lysine coated coverslips were irradiated and returned to 37°C. After 1 h of irradiation, cells were washed in phosphate buffered saline (PBS), fixed for 15 min in 2% paraformaldehyde and washed again in PBS. Subsequently, cells were permeabilized for 5 min with 0.5% Triton X-100 solution in 100 mM Tris, 50 mM EDTA and washed with PBS. Finally the cells were blocked at 4°C overnight in PBG solution (phosphate buffer, 0.5 % BSA fraction V, 0.2 % Gelatin).

For immunofluorescence staining of γ-H2AX, we used a mouse monoclonal antibody (clone 3F2, Abcam) at 1:200 dilution in PBG. Cells were incubated for 90 min with the primary antibody and were washed three times for 5 min in PBS. Then the secondary antibody (anti-mouse Alexa488, Invitrogen) was added for 60 min and samples were washed again three times. Samples were counterstained for 15 min with 50 ng/ml DAPI and mounted on microscope slides with Prolong-Gold Antifade solution (Invitrogen) before scanning in a Leica TCS SP5 confocal microscope.

For digital image analysis the ImarisXT 6.0 software (Bitplane) was used. With the 'spots' and 'split-spots' functions of this software, foci numbers were calculated in the three dimensional image stacks generated. Only objects with a minimum diameter of 0.5 μm after thresholding were counted as foci. For every dose ~150 cells were quantified.

RESULTS

Similar induction of labile lesions in G1 and G2 phases of the cell cycle

Previous studies (19–21,36) and our recent work (26) show that exposure of mammalian cells to IR induces lesions in the DNA, which although in their initial form are not disrupting the sugar–phosphate backbone they do so after chemical processing at 50°C. When present within a CDS, these lesions contribute to the formation of excess DSBs, detected by the difference in the yield between HTL and LTL measurements. This difference is cell line dependent, which suggests biological determinants in the formation of thermally labile lesions (26). If these biological determinants also have a cell cycle component, they will confound the interpretation of results obtained with asynchronous cells (37). Therefore, we analyzed using HTL and LTL the radiation yields of DSBs in enriched G1 and G2 populations of *LIG4*$^{-/-}$ MEFs and compared the results to those previously obtained with asynchronous cells (Supplementary Figure S1).

It is evident from the difference in the slopes of dose–response curves with asynchronous cells that the yield of prompt DSBs and of DSBs generated by chemical processing at 50°C of labile lesions are approximately equal. Similar ratios of prompt and heat labile DSBs are also measured in populations irradiated in the G1 and G2 phase of the cell cycle. This result combined with the abundance of S-phase cells in exponentially growing populations, rules out strong cell cycle effects in the generation of DSBs from labile lesions. Similar conclusions are drawn from experiments carried out with *Ku70*$^{-/-}$ MEFs (Supplementary Figure S2). Therefore, further experiments were carried out with asynchronous cell populations.

Preservation of labile DNA lesions with unchanged thermal lability after LTL

If DNA lesions transforming to DSBs at 50°C remain stable in a cell incubated at 37°C, the excess DSBs detected after HTL in the above experiments will never form in cells maintained under physiological conditions and DNA integrity will be restored by pathways other than those utilized to process DSBs (19–21,36). However, the response reported for plasmid DNA (6,11–13) suggests sensitivity of these lesions to lower, more physiological temperatures and therefore also to temperatures typically used to grow and maintain mammalian cells. To explore this possibility we studied first their stability in cellular DNA after LTL, and second their lability to a subsequent incubation at high temperature.

For this purpose, *LIG4*$^{-/-}$ cells were irradiated and processed by LTL immediately thereafter (flow diagram in Figure 1). The resulting agarose blocks were then incubated for different times at different temperatures in TEN buffer and directly analyzed by PFGE, as additional lysis was not required. Incubation at 50°C causes a strong increase in FDR with a half time of about 3 h. FDR approaches a plateau at 8 h at levels slightly lower than those measured after HTL (Figure 1). Thus, labile DNA lesions are conserved during lysis at low temperature and contribute to DSB formation after post-lysis exposure to 50°C. Similar results are obtained with *M059K* cells (Supplementary Figure S3), and in this case the plateau is actually reached at levels slightly higher than those of HTL. With both cell lines, increase in FDR at 50°C is only observed in irradiated cells and is absent in non-irradiated cells (Figure 1 and Supplementary Figure S3).

The preservation of labile lesions in irradiated DNA after LTL and their contribution to DSBs after post-lysis *in vitro* incubation at 50°C, generates a useful system for analysing their stability at the more physiological temperature of 37°C (Figure 1). Notably, incubation of

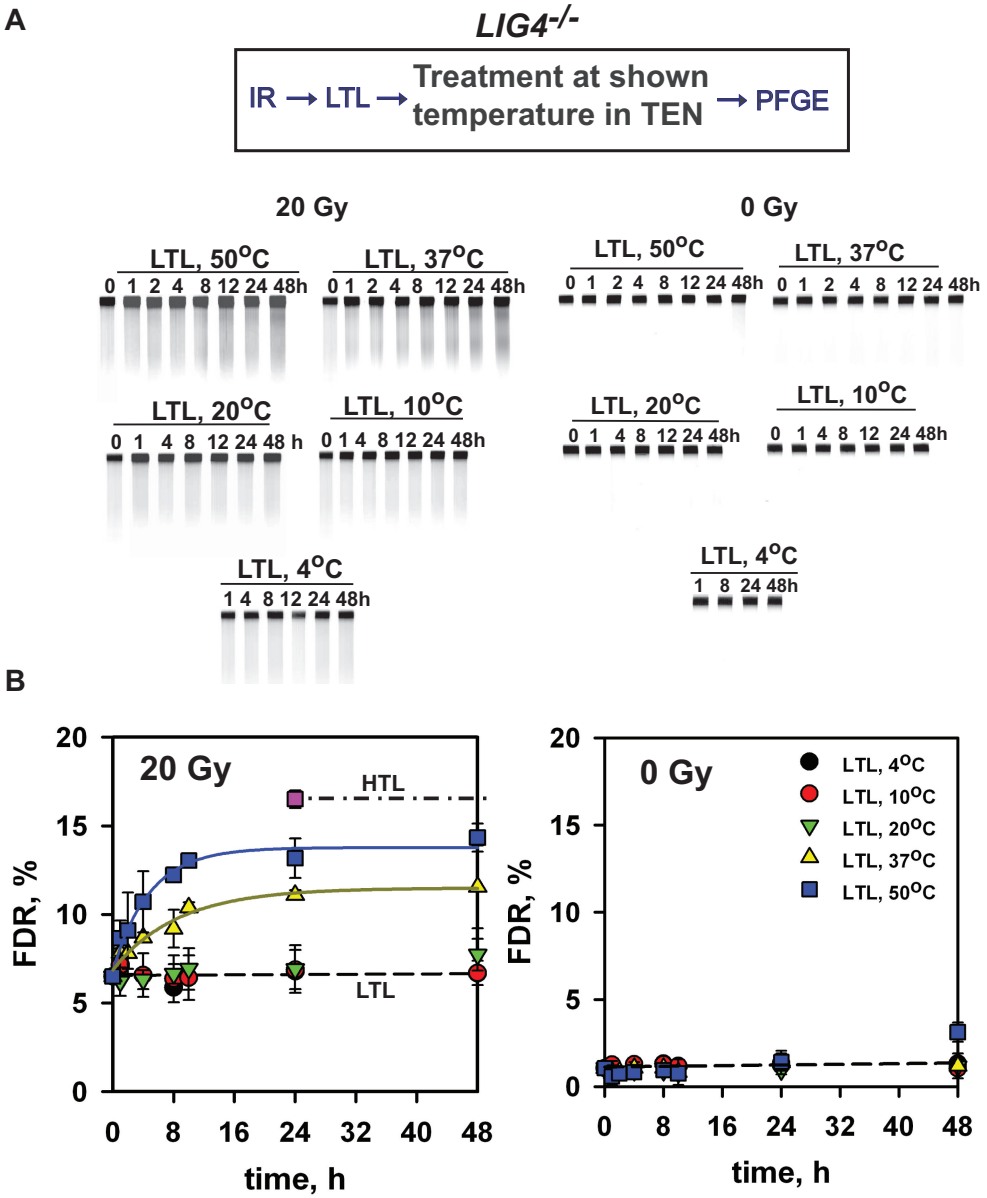

Figure 1. Generation of excess DSBs after *in vitro* incubation of DNA from irradiated cells at different temperatures. *LIG4*$^{-/-}$ MEFs were embedded in agarose, exposed to 20 Gy X-rays and subjected to LTL as described under 'Materials and Methods' section. Subsequently, agarose blocks were incubated at different temperatures for different periods of time in TEN-buffer before analysis for DSBs by PFGE. (**A**) Shows typical ethidium bromide stained gels of irradiated and non-irradiated samples at the different treatment conditions. (**B**) Shows change in FDR as a function of time at the different incubation temperatures for samples exposed to IR, as well as for the corresponding non-irradiated controls. The observed increase in FDR reflects an increase in the formation of DSBs during the period of *in vitro* incubation caused by the conversion of labile lesions to DSBs. Results shown represent the mean and standard error calculated from six determinations in two experiments.

similarly irradiated agarose blocks at 37°C also causes a large increase in FDR, albeit with slower kinetics and reaching final levels slightly lower than after incubation at 50°C. Qualitatively similar results are obtained with *M059K* cells (Supplementary Figure S3), but notably, in this cell line incubation at 37°C and 50°C has similar final effect that is comparable to that seen after HTL. In contrast to observations at 37°C and 50°C, labile lesion conversion and excess DSB formation are not observed after incubation at temperatures ranging between 4°C–20°C (Figure 1 and Supplementary Figure S3).

To investigate possible overlap between lesions converted to DSBs after DNA incubation at 37°C and 50°C, we carried out experiments in which agarose blocks of irradiated *LIG4*$^{-/-}$ MEFs lysed by LTL were exposed in tandem to different temperatures. The results in Supplementary Figure S4 show that compared to 24 h incubation at 50°C, 24 h incubation at 37°C gives a lower FAR that increases slightly after incubation at 37°C for 48 h (Figure 1). Incubation at 37°C for 24 h in tandem with incubation for 24 h at 50°C causes no FAR increase beyond the values measured after 50°C

incubation alone. This suggests that no lesions beyond those already converted at 50°C are affected by incubation at 37°C. In tandem incubation at 37°C for 48 h and 50°C for 24 h leads to FAR higher than that measured after 24 h at 50°C suggesting that additional subsets of lesions exist that convert to DSBs after harsher treatments. We return to this point later.

Chromatin organization is not prerequisite for the formation of labile DNA lesions

In the above experiments, damage was induced by IR in chromatin-organized DNA. However, the extent and possibly also the nature of damage induced by IR in the DNA is known to depend on the degree of this packaging. The presence of histones and other chromatin associated proteins changes the chemical environment of the DNA and may reduce its accessibility to radiation-induced free radicals [(20,38,39) and references therein], or increase accessibility of reducing agents. To test the role of chromatin organization in the formation of radiation-induced labile lesions and connect our observations to those previously reported with purified DNA ('Introduction' section), we irradiated agarose blocks containing DNA prepared by LTL from non-irradiated cells (Figure 2A). Under our experimental conditions, IR induces in 'naked' DNA nearly five times more DSBs than in DNA irradiated in intact cells (Supplementary Figure S5). There is no increase in FDR when agarose blocks are maintained either at 4°C, 10°C or 20°C. Incubation, on the other hand, at 50°C causes a pronounced increase in FDR that reaches a plateau at 24 h. Notably, incubation at 37°C causes again an increase in FDR only slightly slower and only ~20% lower than that observed at 50°C. In non-irradiated DNA, incubation at high temperatures has no detectable effect on DNA integrity (Figure 2A). Similar conclusions can be drawn from experiments carried out with *M059K* cells (Supplementary Figure S6). Thus, as reported previously (19,20), labile lesions are efficiently produced after irradiation of DNA organized in chromatin, as well as after irradiation of 'naked' DNA.

Protein accelerates the thermal conversion of radiation lesions

The above results suggest that excess DSBs will form in the repairing cell by the transformation of heat labile radiation lesions. The conversion kinetics measured when irradiated DNA is incubated at 37°C suggests a time frame of 12–24 h for this conversion. We inquired whether the conversion kinetics is modified when chromatin organization is partly maintained during the post-irradiation incubation period. Indeed, early work suggests alterations in the spectrum of radiation-induced labile lesions in the presence of protein (40). For this purpose, we embedded in agarose irradiated, *LIG4*$^{-/-}$ MEFs and processed them using a protocol previously developed to analyze repair kinetics throughout the cell cycle using cell sorting (33). The protocol effectively stops all cellular metabolic functions including DSB repair—an essential requirement in these experiments—but preserves cellular form and integrity including global nuclear organization. These agarose blocks were then incubated for various periods of time at different temperatures and analyzed by PFGE after LTL. It is evident (Figure 2B) that under these conditions the conversion of thermally unstable lesions to SSBs is much faster than in 'naked' DNA, as indicated by the rapid increase in FDR, reaching a plateau after 1 h at 50°C, and after 2 h at 37°C. While several interpretations are possible for this result, our working hypothesis is that the presence of protein accelerates the chemical modification to DSBs of radiation-induced labile lesions. Furthermore, since even the protocol used here causes extensive protein extraction and protein denaturation, we postulate that in the intact cell this conversion will occur even faster.

Total DSBs are detected by the DDR apparatus shortly after IR

To extract further information on the 37°C transformation of radiation-induced labile lesions, we scored γ-H2AX foci in G1 cells obtained by elutriating logarithmically growing CHO cultures (Figure 3). It is widely accepted that the number of γ-H2AX foci scored 30–60 min after IR reflects the number of DSBs detected by the cellular DDR system (41).

We previously employed this CHO cell line to carefully calibrate throughout the cell cycle the AFIGE signal (FDR) to the average number of DSBs generated in cells by decay of incorporated ^{125}I-dUrd (42). We were therefore keen to use the result of this calibration for the purpose of the present work. Although the calibration was carried out using HTL, induction of additional DSBs from labile lesions is not expected after ^{125}I decay. According to this calibration, exposure of cells to 1 Gy X-rays will induce 10.5 prompt DSBs and 21 total DSBs. This calculation assumes that the difference by a factor of two between prompt and total DSBs measured for MEFs (Supplementary Figures S1 and S2) also holds for CHO cells.

We compared this estimated number of DSBs with the number of γ-H2AX foci actually scored in G1-CHO cells (Figure 3). The results show good agreement between γ-H2AX foci scored at 1 h and the total number of DSBs expected. We conclude that the DSB pool detected by the cell includes both prompt and delayed DSBs; and that the generation of delayed DSBs is largely completed within the 30–60 min required for the development of the signaling cascades that culminate with the phosphorylation of H2AX (Section 1 of Supplementary 'Text').

If conversion of thermally unstable lesions occurs within ~1 h from radiation exposure, one would expect that in repairing cells the dependence of FAR on lysis conditions would diminish with progressing incubation time. Supplementary Figure S7 summarizes such data extracted from repair kinetics measured either after HTL or LTL (26). It is evident that with all cell lines examined the difference in FAR becomes small or negligible after 1 h. This is in agreement with a conversion of labile lesions to DSBs within 1 h. However, the results are also compatible with fast repair of non-DSB lesions within the CDS that

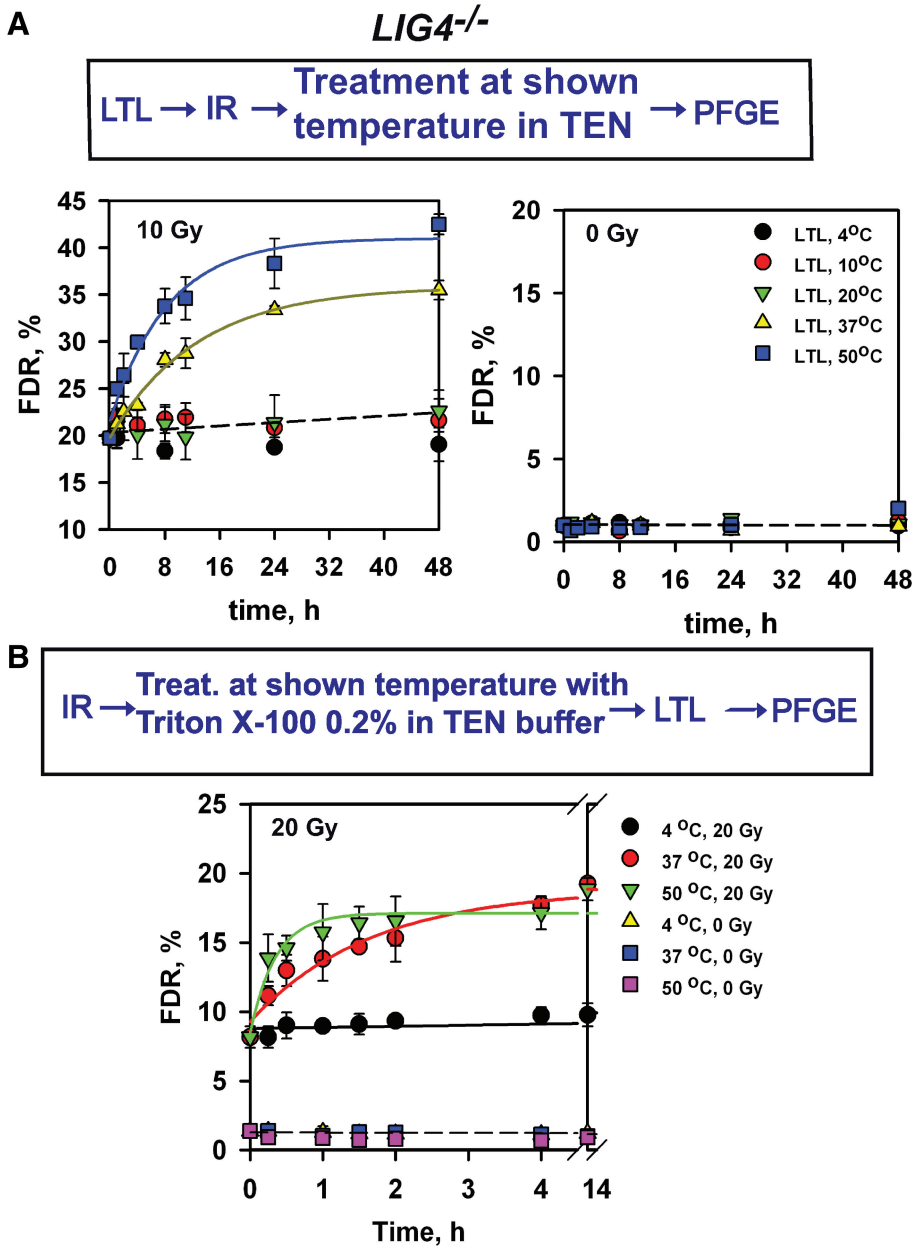

Figure 2. (**A**) Generation of excess DSBs after incubation at different temperatures and for different periods of time of DNA prepared by LTL from non-irradiated cells. *LIG4*$^{-/-}$ MEFs were embedded in agarose blocks, subjected to LTL as described under 'Material and Methods' section and exposed to 10 Gy X-rays. Subsequently, agarose blocks were incubated in TEN-buffer at different temperatures and for different periods of time as indicated. Other details as in Figure 1. Results shown represent the mean and standard error calculated from six determinations in two experiments. (**B**) Generation of excess DSBs after incubation at different temperatures and for different periods of time chromatin organized DNA of irradiated cells. *LIG4*$^{-/-}$ MEFs were embedded in agarose, exposed to 20 Gy X-rays and transferred immediately in TEN-buffer supplemented with 0.2% Triton X-100. This treatment stops all cellular metabolic activities, including DSB repair, but retains cellular integrity including global nuclear architecture. Agarose blocks were then incubated in the same buffer at different temperatures for different periods of time and were, subsequently, lysed by LTL. Other details as in Figure 1. Results shown represent the mean and standard error calculated from six determinations in two experiments.

prevents the formation of a DSB upon the chemical processing of the labile radiation lesion.

Radiation-induced labile lesions evolve by oxidation

The chemical identity of the radiation-induced labile lesions that contribute to the formation of excess DSBs remains unknown and cannot be determined in experiments of the kind reported here. We sought therefore to define instead aspects of the chemical environment that modulate this chemical evolution. First, we examined their stability in a reducing environment generated by 2 mM DTT using the treatment protocols employed in the experiments described in Figure 1.

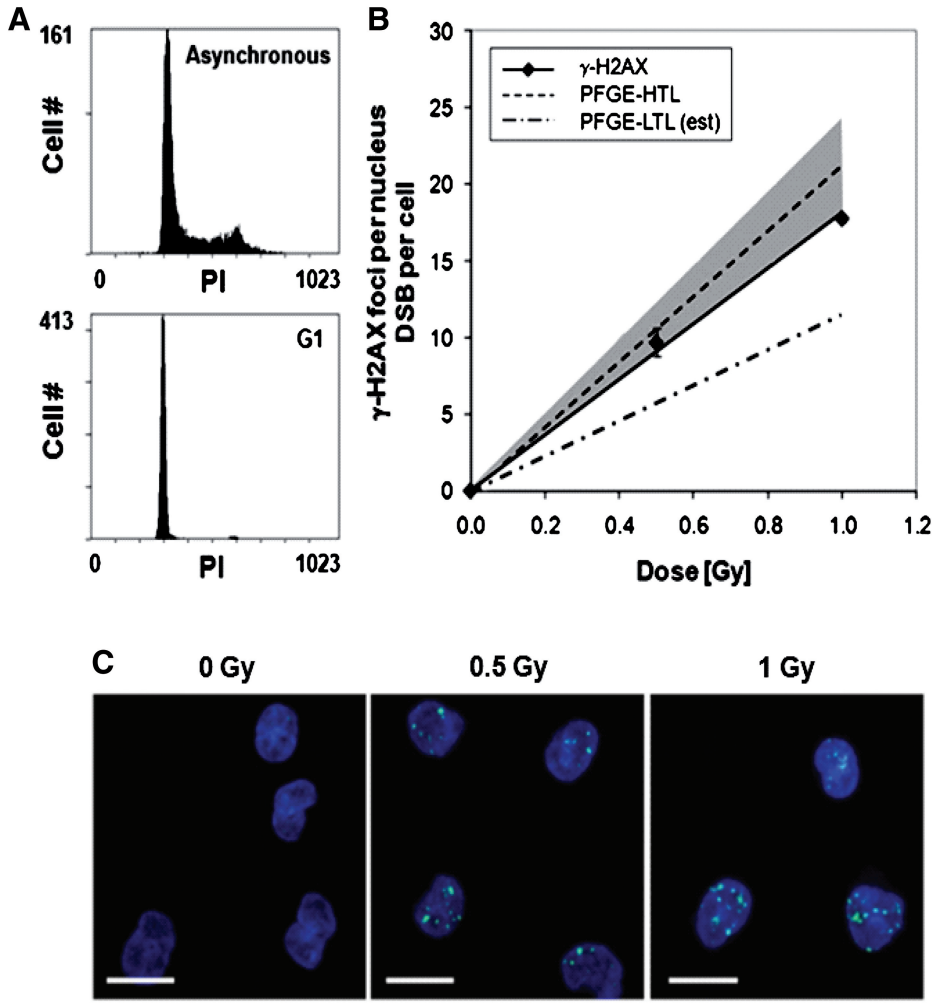

Figure 3. The yield of γ-H2AX foci in irradiated cells corresponds to the sum of DSBs induced promptly and those induced in a delayed manner as a result of conversion to DSBs of labile lesions within a CDS. (**A**) Exponentially growing CHO cells, upper panel, were elutriated to obtain a highly enriched (98%) G1 cell population, lower panel. (**B**) An enriched G1 population of CHO cells was analyzed using confocal laser scanning microscopy for γ-H2AX foci 60 min after exposure to the indicated doses of IR. The solid line shows the best fit though the measured data points. The shaded area defines the range (±10%) of total DSB induction calculated using the calibration in G1 phase previously carried out using ^{125}I decay (42). The lower broken line is the estimated yield for the induction of prompt DSBs as measured by LTL assuming a ratio of LTL versus HTL similar to that measured for *LIG4*$^{-/-}$ MEFs in Supplementary Figure S1. (**C**) Shows representative images of CHO cells exposed to the indicated doses of radiation in nuclei counterstained with DAPI. Scale bars are 10 μm.

The results obtained (Figure 4) show complete thermal stability for these lesions in a reducing environment, even when incubated at 50°C for up to 48 h. Similar results were obtained in a similar experiment using β-mercaptoethanol (Supplementary Figure S8). We interpret these results as evidence that the chemical evolution of radiation-induced labile lesions occurs by oxidation, which is accelerated with increasing incubation temperature.

To examine the effect of protonation on the evolution of radiation-induced labile DNA lesions, we analyzed the effect of 100 mM lysine in a similar experiment. The results (Figure 5) indicate that under these conditions lesion lability increases. Thus, significant formation of excess DSBs is observed after incubation at 4°C and 20°C, which are otherwise preserving labile lesions. At 37°C and 50°C the formation of excess DSBs is enhanced with more DSBs forming than after HTL. This result suggests that HTL uncovers only a subset of radiation-induced labile lesions and is in line with results obtained after tandem treatments of DNA at different temperatures (Supplementary Figure S4). It follows that radiation-induced labile lesions that convert to DSBs do not represent a single chemical species, but rather a spectrum of lesions with different reactivity and thus also different thermal stability.

Thermally unstable lesions are not base damages or AP sites recognized by Fpg or Nth

It is possible that thermally unstable lesions represent base damages and/or apurinic or apyrimidinic sites of the form that can be recognized by Fpg or Nth endonucleases (16,17,34,43,44). To investigate this possibility, we embedded into agarose cells exposed to 0 or 20 Gy, lysed

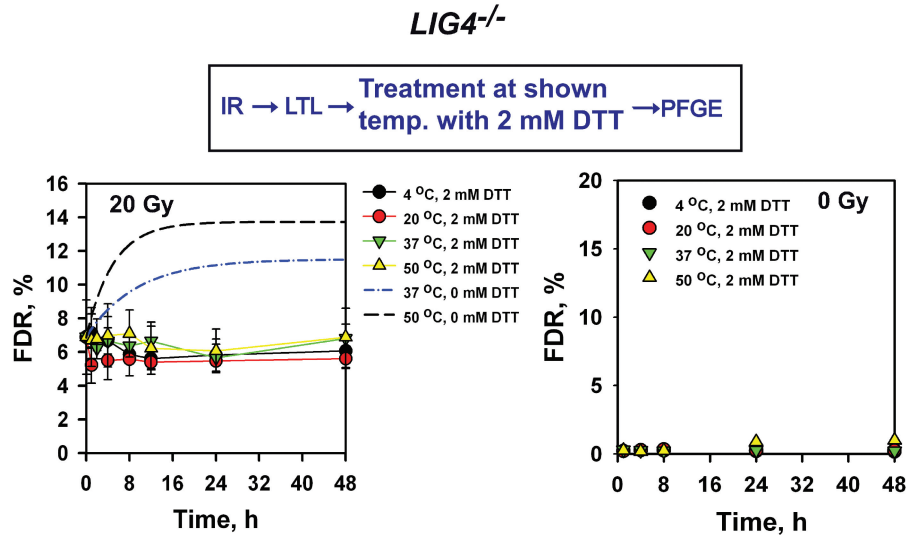

Figure 4. The conversion to DSBs of radiation-induced labile DNA lesions is drastically diminished in a reducing environment. *LIG4*$^{-/-}$ MEFs embedded in agarose were exposed to 20 Gy X-rays, subject to LTL and treated at different temperatures for different periods of time in TEN buffer supplemented with 2 mM DTT. Other details as in Figure 1. The dotted lines show the response of samples incubated in TEN in the absence of DTT and have been transferred from Figure 1. Results shown represent the mean and standard error calculated from six determinations in two experiments.

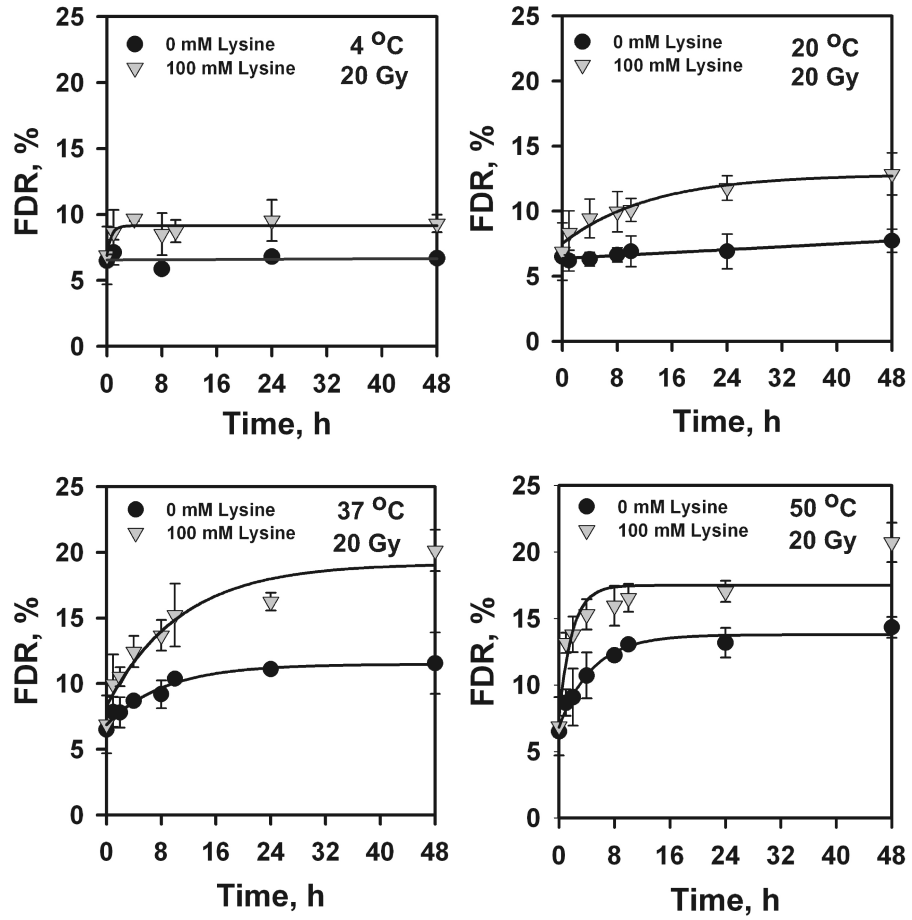

Figure 5. L-lysine enhances the conversion to SSBs of radiation-induced labile DNA lesions. LIG4$^{-/-}$ MEFs embedded in agarose were exposed to 20 Gy X-rays, subjected to LTL and treated at different temperatures for different periods of time in TEN-buffer supplemented with 100 mM L-lysine. The different panels show results obtained at the different temperatures after incubation in the presence or absence of L-lysine. The results without L-lysine have been transferred from Figure 1. Results shown represent the mean and standard error calculated from six determinations in two experiments.

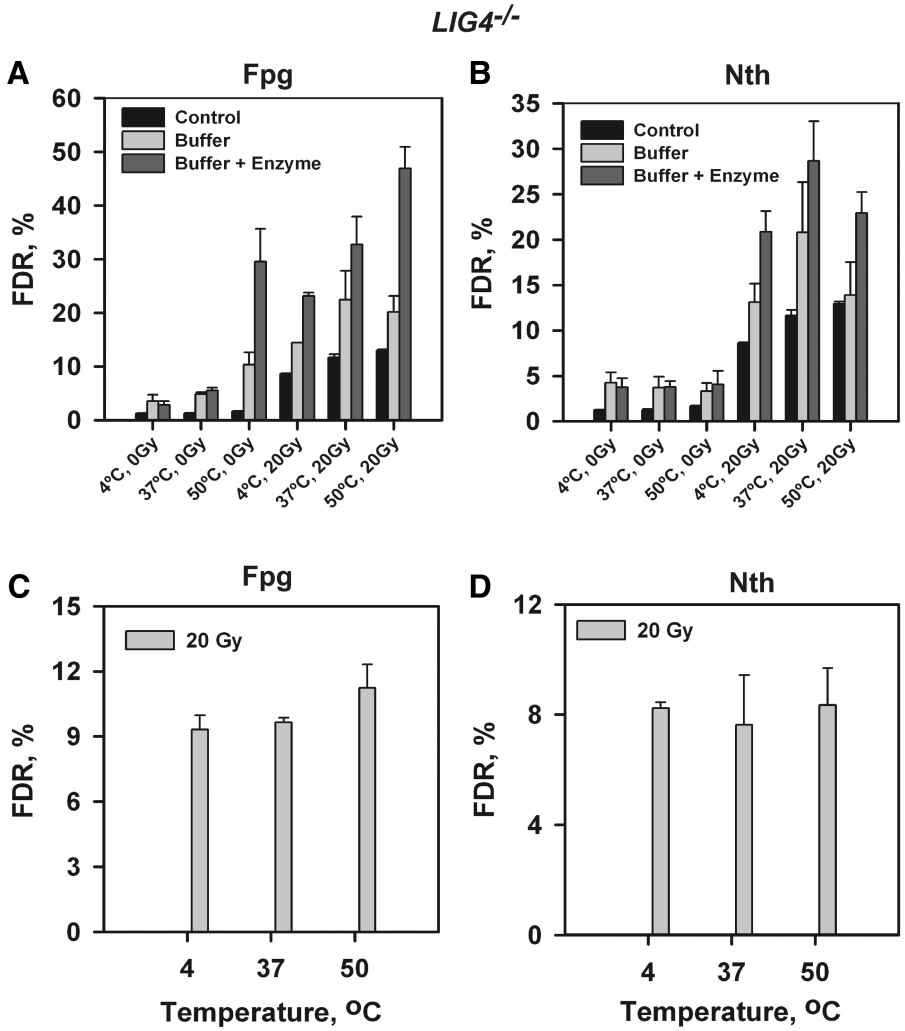

Figure 6. Apurinic or apyrimidinic sites are unlikely to represent radiation-induced labile lesions. LIG4$^{-/-}$ MEFs embedded in agarose were exposed to 20 Gy X-rays and subjected to LTL. Subsequently, agarose blocks were incubated at 4, 37 and 50°C for 48 h and then treated with 400 ng/plug Fpg or 1.2 μg/plug Nth for 24 h at 20°C before analysing by PFGE. (**A**) FDR measured at the different treatment conditions as indicated. Control: samples maintained in TEN-buffer throughout. Buffer: samples maintained in enzyme buffer during the enzyme treatment step. Buffer + enzyme: samples maintained in enzyme buffer with the indicated amount of Fpg during the enzyme treatment step. (**B**) As is A but for Nth. (**C**) Net increase in FDR as a result of Fpg treatment in irradiated samples pre-treated as indicated. Net increase was calculated by subtracting the FDR of buffer-only samples from that obtained in the presence of the enzyme. (**D**) Same as in **C** but for Nth.

them by LTL and incubated the resulting blocks for 48 h in TEN at 4°C, 37°C or 50°C to achieve the corresponding transformation to SSBs of thermally unstable lesions. These agarose blocks were, subsequently, incubated for 24 h at 20°C (which preserves labile lesions according to the results shown in Figure 1) in the presence of either 400 ng/plug Fpg or 1.2 μg/plug Nth and the DSB load analyzed by PFGE. In Figure 6A and B show actual FDR values of samples treated as indicated with Fpg and Nth, respectively. Figure 6C and D show net FDR increases in enzyme treated samples. It is evident that the net increase in FDR as a result of Fpg or Nth treatment is comparable in all sets, irrespectively of whether or not DNA was pre-treated at high temperatures to force the evolution of labile lesions to DSBs. This observation suggests that thermally unstable lesions causing DSBs are not lesions recognized by Fpg or Nth and is in line with observations with DNA in solution (45). Base damages and AP-sites recognized by these endonucleases are actually retained within the CDS and are converted to DSBs after enzyme treatment with the same efficiency in samples incubated at 4°C, 37°C or 50°C.

DISCUSSION

The role of radiation-induced labile lesions in the yield of DSBs in vertebrate cells

Several reports in the last 30 years pointed out the generation in *in vitro* irradiated DNA of chemically labile lesions with the unique characteristic of not disrupting initially the sugar–phosphate backbone, but of doing so after chemical processing—which is accelerated by high

temperature or pH. Surprisingly, the ramifications of these observations in the experimental quantitation and processing of DSBs were rarely considered.

Recently, problems in the quantitation of DSBs by PFGE utilizing HTL were pointed out by Rydberg (19) and Stenerlöw *et al* (20). It was shown that >40% of the DSBs measured by HTL immediately after IR form during lysis from the conversion of labile lesions, and that these DSBs are not actually present in the tested cells. Assuming that conversion to DSBs requires temperatures in the vicinity of 50°C, the authors concluded that these lesions will be stable and will never convert to DSBs in the repairing cell. Their detection by PFGE will stop when lesions other than these labile sites are removed from the CDS by non-DSB repair pathways. Thus, repair of non-DSB lesions will be 'detected' as DSB repair. This reasonable scenario was questioned by the observation that repair of these 'artifactual' DSBs is independent of PARP-1 or XRCC1, two strong candidate components for the repair of SSB and base damage within the CDS (21). While the latter result could reflect repair by pathways not requiring these activities (46), it also suggests that alternative possibilities regarding the fate of these lesions inside the cell should be considered.

While our recent results (26) and the results presented here confirm that in vertebrate cells 40–60% of the DSBs measured immediately after IR are artifactually generated during HTL, they also demonstrate that these labile lesions are sensitive to the physiological temperature of 37°C. This observation raises this subset of DSBs from a method-related artifact to an entity with potentially important biological consequences.

If this subset of DSBs also develops in repairing cells, their gradual formation will continuously modify the damage load of the cell. From previous estimates (12,19,20) and our results, this production half time is about 3 h when protein-free DNA is exposed to 50°C. If this relatively slow rate of conversion were maintained in cells at 37°C, the biological consequences of the resulting DSBs might have been limited for two reasons. First, only relatively few DSBs would be added to the total load at any time, and second, the formation of these extra DSBs might have been prevented all together by repair before labile-site conversion, of other lesions within the CDS by non-DSB repair pathways.

It is therefore particularly relevant that the conversion of radiation-induced labile lesions to DSBs is accelerated in protein-associated DNA, reaching half maximum times of about 1 h (Figure 2B). Since even this experiment includes extensive protein extraction by Triton X-100, which frees-up cells from the bulk of unbound protein, we anticipate even faster conversion kinetics in intact cells.

As a first test of this postulate, we compared the DSB load detected by the cellular DDR system in the form of γ-H2AX foci with the load of DSBs detected by PFGE, either after LTL to reflect prompt DSBs, or after HLT to reflect the total load including both prompt and heat labile DSBs (Figure 3). Notably, these experiments were carried out with a CHO cell line where PFGE was independently calibrated, and were using G1 cells to avoid cell cycle artifacts. The similarity between the number of γ-H2AX foci scored and the total number of DSBs measured is interpreted as evidence, albeit indirect, that radiation-induced labile sites contribute to DSB induction within the 30–60 min required by the cell to fully activate its DDR system.

Thus, DSBs originating from radiation-induced labile lesions are not only artifactually generated during HTL, but are a reality the irradiated cell faces during physiological incubation conditions. We propose that this 'late forming' subset of DSBs adds to those promptly induced and generates the total load detected by the DDR apparatus. As a result, the total DSB load a cell detects after IR includes for the most part both those promptly induced, as well as those late forming as a result of labile lesion conversion.

This postulate allows re-interpretation of the kinetics of DSB repair occasionally measured in D-NHEJ deficient cells after LTL (Figure 7). The slight increase in FDR

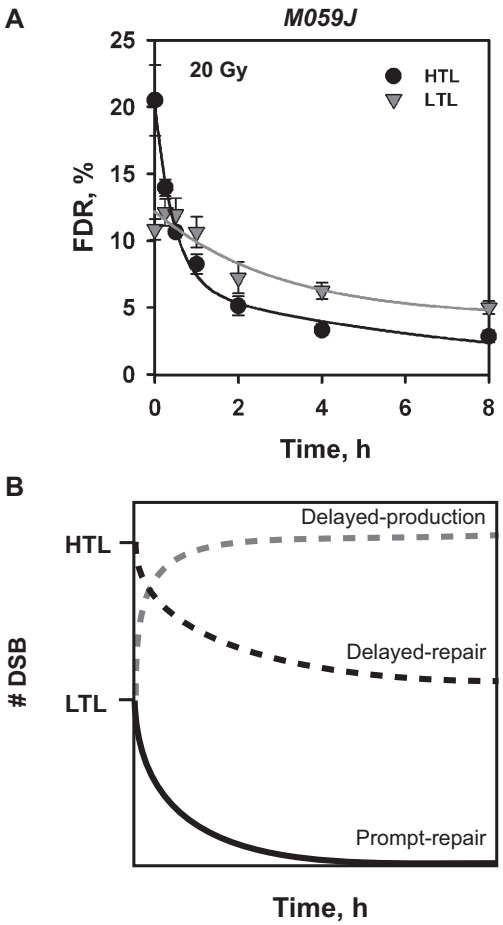

Figure 7. (**A**) Repair kinetics in M059J cells as measured after LTL and HTL. (**B**) Schematic description of processes that can lead to the kinetics of DSB repair shown by the gray line in A. Three distinct processes are envisioned. First, prompt DSBs, which are present immediately after irradiation, are repaired with the indicated kinetics. Second, delayed DSBs generated from radiation-induced labile lesions are not present immediately after IR, but are generated soon thereafter reaching a plateau at about 1 h post-irradiation. These newly formed DSBs are repaired as they arise (see text for details).

reproducibly observed at early times in these experiments is compatible with the transformation to DSBs of labile sites at a rate overtaking overall DSB repair in this repair deficient background. According to this interpretation, a DSB repair curve reflects at a minimum the sum of the following processes (Figure 7B): (i) repair of prompt DSBs through known pathways and processes; (ii) formation of delayed DSBs from the conversion of radiation-induced labile lesions; (iii) repair of DSBs produced by the latter process. It remains to be established whether the delayed generation of the latter subset of DSBs has adverse consequences for their processing. For example, a prompt SSB within a CDS containing a thermally unstable lesion may be immediately recognized as such initiating SSB-related cellular signaling, including PARP1 activation and poly(ADP)ribosylation. Formation of a DSB in this already pre-processed SSB region of the DNA will abruptly alter the signaling and processing requirements and will force them towards those appropriate for a DSB. This sudden and radical change in lesion identity may generate signaling 'conflicts' that will affect the processing of the resulting DSB.

The above model may be extended to include the generation of DSBs through the enzymatic processing of base damage within a CDS (16,17,34,36,43), as well as the possible elimination of potential DSBs by the rapid enzymatic removal of SSBs or base lesions within the CDS that will preclude the generation of a DSB from a converted labile lesion (21,36). Quantitative experimental description of the sum of all these processes will require mathematical modeling combined with appropriate genetic systems.

The slightly reduced repair after LTL observed in Figure 7 after long incubation times is specific for M059J cells and not detectable in other D-NHEJ deficient cells (26). It may reflect experimental uncertainties, incomplete lysis or other unknown effects.

Radiation-induced labile lesions evolve by oxidation

The stability of radiation-induced labile lesions in a reducing environment even at high temperatures (Figure 4 and Supplementary Figure S8) implicates oxidation as a key reaction in their chemical evolution. The immediate lesion environment is a key determinant for this oxidation, as indicated by the observation that bound protein accelerates the process.

The increased lability and conversion to DSBs of labile sites in the presence of L-lysine (Figure 5) shows not only that conversion can be chemically accelerated, but also that there are more labile lesions present in the cell than are actually converted to DSBs after incubation at high temperature. The differences in stability point to a spectrum of lesions, rather than a single lesion, that awaits chemical characterization and quantitative consideration in radiation response.

The possibility of enhancing the stability of labile radiation lesions by providing a reducing environment opens the theoretical possibility of protecting irradiated cells by modulating in a targeted manner their conversion to SSBs. Similar arguments can be developed for their oxidation and the potentially associated sensitization.

It has been demonstrated that IR induces 4–5 times more CDSs containing base lesions than frank DSBs (8,9). These CDS can be converted to DSBs by the simultaneous opening of both DNA strands during repair (16,17,34,36,43). The overrepresentation of this form of CDS in irradiated cells, opens the possibility that the observed radiation-induced labile sites partly reflect this from of damage. However, the results presented in Figure 6 demonstrate that the subset of lesions that can contribute to the DSB load through enzymatic conversion and those contributing through chemical conversion are distinct and their effects in the experiments described here additive. This conclusion is in line with observations with *in vitro* irradiated DNA (45), and with the fact that AP sites have longer half times than radiation-induced labile lesions at 50°C (44).

Implications for DDR of the intracellular chemical evolution of labile lesions

Labile lesions increasing the DSB load in a cell already engaged in repair add yet another parameter to the already complex pattern of DNA damage induction, detection and processing in an irradiated cell. DSBs thus generated may be subject to constraints in terms of signaling and repair that are different from those of promptly generated DSBs. Several questions arise: (i) if enzymatic repair of SSBs and base damages within a CDS containing a labile lesion starts before its conversion to a break, will the proteins already recruited to the site before this conversion impair signaling from and processing of the DSB generated after its chemical conversion? (ii) How are DTT and β-mercaptoethanol enhancing the stability of these lesions? What type of sugar lesion underlies this effect? (iii) *In vitro* experiments have shown that the same subset of radiation-induced labile lesions shows increased sensitivity to increased temperature and to alkali (11). Is this also true for lesions induced by IR in intact cells as shown here? (iv) How is the formation of labile lesions, as well as the induction of the associated DSBs affected by the LET of the radiation used? Only additional work will address these and many other important questions and will shed light on the role of these intriguing lesions in the cellular response to IR.

SUPPLEMENTARY DATA

Supplementary Data are available at NAR Online.

ACKNOWLEDGEMENTS

The authors are indebted to Fred Alt and David Chen for cells.

FUNDING

The European Space Agency (ESA) (AO-08-IBER) and the Bundesministerium für Bildung und Forschung (BMBF), Kompetenzverbund Strahlenforschung (KVSF)

(02NUK005C, 02NUK001B). Funding for open access charge: BMBF.

Conflict of interest statement. None declared.

REFERENCES

1. Goodhead,D.T. (1994) Initial events in the cellular effects of ionizing radiations: clustered damage in DNA. *Int. J. Radiat. Biol.*, **65**, 7–17.
2. von Sonntag,C. (1987) *The Chemical Basis of Radiation Biology*. Taylor and Francis, London-New York-Philadelphia.
3. von Sonntag,C. (2006) *Free-Radical-Induced DNA Damage and Its Repair*. Springer, Berlin-Heidelberg, Germany.
4. Friedberg,E.C., Walker,G.C., Siede,W., Wood,R.D., Schultz,R.A. and Ellenberger,T. (2006) *DNA Repair and Mutagenesis*, 2nd edn. ASM Press, Washington, DC, USA.
5. Ward,J.F. (1985) Biochemistry of DNA lesions. *Radiat. Res.*, **104**, S103–S111.
6. Ward,J.F. (1988) DNA damage produced by ionizing radiation in mammalian cells: Identities, mechanisms of formation, and reparability. *Prog. Nucleic Acid Res.*, **35**, 95–125.
7. Brenner,D.J. and Ward,J.F. (1992) Constraints on energy deposition and target size of multiply damaged sites associated with DNA double-strand breaks. *Int. J. Radiat. Biol.*, **61**, 737–748.
8. Georgakilas,A.G. (2008) Processing of DNA damage clusters in human cells: current status of knowledge. *Mol. BioSyst.*, **4**, 30–35.
9. O'Neill,P. and Wardman,P. (2009) Radiation chemistry comes before radiation biology. *Int. J. Radiat. Biol.*, **85**, 9–25.
10. Jackson,S.P. and Bartek,J. (2009) The DNA-damage response in human biology and disease. *Nature*, **461**, 1071–1078.
11. Lafleur,M.V.M., Woldhuis,J. and Loman,H. (1979) Alkali-labile sites and post-irradiation effects in gamma-irradiated biologically active double-stranded DNA in aqueous solution. *Int. J. Radiat. Biol.*, **36**, 241–247.
12. Jones,G.D., Bowell,T.V. and Ward,J.F. (1994) Effects of post-irradiation temperature on the yields of radiation-induced single- and double-strand breakage in SV40 DNA. *Radiat. Res.*, **138**, 291–296.
13. Henle,E.S., Roots,R., Holley,W.R. and Chatterjee,A. (1995) DNA strand breakage is correlated with unaltered base release after gamma irradiation. *Radiat. Res.*, **143**, 144–150.
14. von Sonntag,C. and Schulte-Frohlinde,D. (1978) Radiation-induced degradation of the sugar model compounds and in DNA. *Mol. Biol. Biochem. Biophys.*, **27**, 204–226.
15. Fung,H. and Demple,B. (2011) Distinct roles of Ape1 protein in the repair of dna damage induced by ionizing radiation or bleomycin. *J. Biol. Chem.*, **286**, 4968–4977.
16. Yang,N., Galick,H. and Wallace,S.S. (2004) Attempted base excision repair of ionizing radiation damage in human lymphoblastoid cells produces lethal and mutagenic double strand breaks. *DNA Repair*, **3**, 1323–1334.
17. Harrison,L., Hatahet,Z. and Wallace,S.S. (1999) *In Vitro* repair of synthetic ionizing radiation-induced multiply damaged DNA sites. *J. Mol. Biol.*, **290**, 667–684.
18. Blöcher,D., Einspenner,M. and Zajackowski,J. (1989) CHEF electrophoresis, a sensitive technique for the determination of DNA double-strand breaks. *Int. J. Radiat. Biol.*, **56**, 437–448.
19. Rydberg,B. (2000) Radiation-induced heat-labile sites that convert into DNA double-strand breaks. *Radiat. Res.*, **153**, 805–812.
20. Stenerlöw,B., Karlsson,K.H., Cooper,B. and Rydberg,B. (2003) Measurement of prompt DNA double-strand breaks in mammalian cells without including heat-labile sites: results for cells deficient in non-homologous end joining. *Radiat. Res.*, **159**, 502–510.
21. Karlsson,K.H., Radulescu,I., Rydberg,B. and Stenerlöw,B. (2008) Repair of radiation-induced heat-labile sites is independent of DNA-PKcs, XRCC1 and PARP. *Radiat. Res.*, **169**, 506–512.
22. Wang,H., Rosidi,B., Perrault,R., Wang,M., Zhang,L., Windhofer,F. and Iliakis,G. (2005) DNA Ligase III as a candidate component of backup pathways of non-homologous end joining. *Cancer Res.*, **65**, 4020–4030.
23. Iliakis,G., Wu,W., Wang,M., Terzoudi,G.I. and Pantelias,G.E. (2007) Backup Pathways of Nonhomologous End Joining May Have a Dominant Role in the Formation of Chromosome Aberrations. In Obe,G. and Vijayalaxmi. (eds), *Chromosomal Alterations*. Springer Verlag, Berlin, Heidelberg, New York, pp. 67–85.
24. Wu,W., Wang,M., Mussfeldt,T. and Iliakis,G. (2008) enhanced use of backup pathways of NHEJ in G_2 in Chinese hamster mutant cells with defects in the classical pathway of NHEJ. *Radiat. Res.*, **170**, 512–520.
25. Iliakis,G. (2009) Backup pathways of NHEJ in cells of higher eukaryotes: cell cycle dependence. *Radiother. Oncol.*, **92**, 310–315.
26. Singh,S.K., Wu,W., Wang,M. and Iliakis,G. (2009) Extensive repair of DNA double-strand breaks in cells deficient in the DNA-PK dependent pathway of NHEJ after exclusion of heat-labile sites. *Radiat. Res.*, **172**, 152–164.
27. Yan,C.T., Boboila,C., Souza,E.K., Franco,S., Hickernell,T.R., Murphy,M., Gumaste,S., Geyer,M., Zarrin,A.A., Manis,J.P. *et al.* (2007) IgH class switching and translocations use a robust non-classical end-joining pathway. *Nature*, **449**, 478–482.
28. Nussenzweig,A. and Nussenzweig,M.C. (2007) A backup DNA repair pathway moves to the forefront. *Cell*, **131**, 223–225.
29. Allalunis-Turner,M.J., Zia,P.K.Y., Barron,G.M., Mirzayans,R. and Day,R.S. III (1995) Radiation-induced DNA damage and repair in cells of a radiosensitive human malignant glioma cell line. *Radiat. Res.*, **144**, 288–293.
30. Frank,K.M., Sharpless,N.E., Gao,Y., Sekiguchi,J.M., Fergson,D.O., Zhu,C., Manis,J.P., Horner,J., DePinho,R.A. and Alt,F.W. (2000) DNA ligase IV deficiency in mice leads to defective neurogenesis and embryonic lethality via the p53 pathway. *Mol. Cell.*, **5**, 993–1002.
31. Ouyang,B.H., Nussenzweig,A., Kurimasa,A., da Costa Soares,V., Li,X., Cordon-Cardo,C., Li,W.-H., Cheong,N., Nussenzweig,M., Iliakis,G. *et al.* (1997) Ku70 is required for DNA repair but not for T cell antigen receptor gene recombination in vivo. *J. Exp. Med.*, **186**, 921–929.
32. DiBiase,S.J., Zeng,Z.-C., Chen,R., Hyslop,T., Curran,W.J. Jr and Iliakis,G. (2000) DNA-dependent protein kinase stimulates an independently active, non-homologous, end-joining apparatus. *Cancer Res.*, **60**, 1245–1253.
33. Wu,W., Wang,M., Wu,W., Singh,S.K., Mussfeldt,T. and Iliakis,G. (2008) Repair of radiation induced DNA double strand breaks by backup NHEJ is enhanced in G2. *DNA Repair*, **7**, 329–338.
34. Yang,N., Chaudhry,M.A. and Wallace,S.S. (2006) Base excision repair by hNTH1 and hOGG1: a two edged sword in the processing of DNA damage in γ-irradiated human cells. *DNA Repair*, **5**, 43–51.
35. Song,J.M., Milligan,J.R. and Sutherland,B.M. (2002) Bistranded oxidized purine damage clusters: induced in DNA by long-wavelength ultraviolet (290–400 nm) radiation? *Biochemistry*, **41**, 8683–8688.
36. Gulston,M., de Lara,C., Jenner,T., Davis,E. and O'Neill,P. (2004) Processing of clustered DNA damage generates additional double-strand breaks in mammalian cells post-irradiation. *Nucleic Acids Res.*, **32**, 1602–1609.
37. Karlsson,K.H. and Stenerlöw,B. (2007) Extensive ssDNA end formation at DNA double-strand breaks in non-homologous end-joining deficient cells during the S phase. *BMC Mol. Biol.*, **170**, 467–476.
38. Xue,L.-Y., Friedman,L.R., Oleinick,N.L. and Chiu,S.-M. (1994) Induction of DNA damage in γ-irradiated nuclei stripped of nuclear protein classes: differential modulation of double-strand break and DNA-protein crosslink formation. *Int. J. Radiat. Biol.*, **66**, 11–21.
39. Magnander,K., Hultborn,R., Claesson,K. and Elmroth,K. (2010) Clustered DNA damage in irradiated human diploid fibroblasts: influence of chromatin organization. *Radiat. Res.*, **173**, 272–282.
40. Lafleur,M.V.M., Pluijmackers-Westmijze,E.J. and Loman,H. (1983) Heat-sensitive radiation damage in single-stranded DNA irradiated in a bacterial extract. *Int. J. Radiat. Biol.*, **44**, 483–488.

41. Kinner,A., Wu,W., Staudt,C. and Iliakis,G. (2008) γ-H2AX in recognition and signaling of DNA double-strand breaks in the context of chromatin. *Nucleic Acids Res.*, **36**, 5678–5694.
42. Iliakis,G.E., Cicilioni,O. and Metzger,L. (1991) Measurement of DNA double strand breaks in CHO cells at various stages of the cell cycle using pulsed field gel electrophoresis: calibrations by means of ^{125}I decay. *Int. J. Radiat. Biol.*, **59**, 343–357.
43. Blaisdell,J.O., Harrison,L. and Wallace,S.S. (2001) Base excision repair processing of radiation-induced clustered DNA lesions. *Radiat. Prot. Dosimetry*, **97**, 25–31.
44. Georgakilas,A.G., Bennett,P.V., Wilson,D.M. and Sutherland,B.M. (2004) Processing of bistranded abasic DNA clusters in γ-irradiated human hematopoietic cells. *Nucleic Acids Res.*, **32**, 5609–5620.
45. Lafleur,M.V.M., Woldhuis,J. and Loman,H. (1981) Alkali-labile sites in biologically active DNA: comparison of radiation induced potential breaks and apurinic sites. *Int. J. Radiat. Biol.*, **39**, 113–118.
46. Godon,C., Cordelieres,F.P., Biard,D., Giocanti,N., Megnin-Chanet,F., Hall,J. and Favaudon,V. (2008) PARP inhibition versus PARP-1 silencing: different outcomes in terms of single-strand break repair and radiation susceptibility. *Nucleic Acids Res.*, **36**, 4454–4464.